JOURNAL OF MATERIALS SCIENCE 10 (1975) 833–845

The mechanical behaviour of polystyrene under pressure

K. MATSUSHIGE, S. V. RADCLIFFE, E. BAER
Departments of Macromolecular Science, and Metallurgy and Material Science, Case Western Reserve University, Cleveland, Ohio, USA

Tensile deformation of polystyrene carried out under pressure up to 4 kbar has shown that the pressure-transmitting fluid (silicon oil) acts as a stress crazing and cracking agent. Unsealed specimens showed a brittle-to-ductile transition at 2.95 kbar, while specimens sealed with Teflon tape and rubber showed the same transition at only 0.35 kbar.

Analysis of the stress-strain curves for the sealed specimens indicated that the pressure dependency of the craze initiation stress differs from that of shear band initiation stress. The brittle-to-ductile transition occurs when the initiation stresses of both processes become equal.

The principal stress for craze initiation showed almost no pressure dependency, suggesting that crazes initiate when the principal stress level of the tensile specimen reaches a critical value irrespective of the applied hydrostatic pressure. Similarly, no pressure dependency was observed for the principal ductile fracture stress. The pressure dependency of yield stress agreed well with a non-linear pressure dependent von Mises yield criterion.

Nomenclature

P, pressure
σ_T, observed tensile stress
σ_{ci}, craze initiation stress
σ_y, upper yield stress
σ_f, fracture stress
σ^1, the first principal stress
$\sigma_{ci}{}^1$, principal craze initiation stress
$\sigma_f{}^1$, principal fracture stress
$\tau_{max}(P)$, maximum shear stress at pressure P
τ_0, maximum shear stress at atmospheric pressure
$\tau_{oct}(P)$, octahedral shear stress at pressure P
τ_0', octahedral shear stress at atmospheric pressure
σ_m, mean normal stress
T, tensile yield stress at atmospheric pressure
C, compressive yield stress at atmospheric pressure

1. Introduction

During the past ten years the effect of a hydrostatic pressure on mechanical properties of polymers has received considerable attention because of increasing interest in the solid state processing of this type of highly compressible viscoelastic material. In 1964, Holliday *et al.* [1] observed a surprising phenomenon: polystyrene which is brittle at room temperature and atmospheric pressure becomes ductile under a hydrostatic pressure of 7.7 kbar. Subsequently, these observations stimulated more detailed studies on this unusual brittle-to-ductile transition; Pugh *et al.* [2] and Biglione *et al.* [3] observed that this transition occurs between 2 and 3 kbar. In order to prevent possible environmental effects by the pressure-transmitting fluid, Pugh sealed the tensile test specimen with rubber and observed that both the unsealed and sealed specimens showed the brittle-to-ductile transition at the same pressure of about 2.8 kbar. However, the specific mechanism for the brittle-to-ductile transition was left as an unsolved problem and to date there is no consistent explanation for why this transition should take place at this particular pressure.

Crazing has been recognized to have an important role in the initial fracture process of amorphous polymers. It is easy to suppose that an application of pressure will cause a significant effect on this phenomenon which requires dilation thus giving rise to void formation. Studies on the craze initiation process in glassy polymers have been carried out mainly in biaxial stress fields such as tension–tension [4], torsion–

© *1975 Chapman and Hall Ltd.*

tension [5], and compression–tension [6], but none of the previous studies have been performed in tension under superimposed hydrostatic pressure which can cover much wider stress ranges. In particular, tensile deformation under pressure is a useful experimental arrangement which can be used to study several proposed criteria for craze initiation [4-7].

Yielding under pressure has been studied much more extensively than crazing and several yield criteria have taken into account the large pressure dependency observed in polymeric solids. Whitney and Andrews [8] and Bowden and Jukes [9] used the Coulomb yield criterion [10] to explain their experimental data, while Sternstein and Ongchin [4] and Bauwens [11] proposed quite similar pressure-modified von Mises criteria. Both types of criteria were constructed to give a linear pressure dependency of yield stress. Recently, a non-linear pressure dependent von Mises citerion was suggested by Raghava *et al.* [12] which fitted well the experimental data in a variety of stress fields.

Pressure has also been shown to significantly affect the tensile fracture behaviour. In general, the fracture strains of crystalline polymers such as polyethylene [2, 13, 14], polypropylene [13], polytetrafluoroethylene [15-17], polychlorotrifluoroethylene [15, 17] and nylon 6:6 [2] are reported to increase with pressure except in the case of polyoxymethylene [18]. On the other hand, the reported pressure dependencies of the fracture strain in glassy polymers such as polycarbonate [15, 16], polymethylmethacrylate [2, 15, 19], and polystyrene [2, 3, 17] are quite different and reported results vary between the experimental investigators. Almost all data have been obtained by neglecting possible environmental effects due to the pressure transmitting fluid, and no definite correlations between the fracture strain or stress and the applied pressure have been found.

The present paper is concerned with the mechanism of the brittle-to-ductile transition in polystyrene and the criteria for craze initiation, yielding and ductile fracture under pressure. Special emphasis is placed upon determining the effect of environment on the mechanical properties due to sample immersion in the pressure transmitting fluid.

2. Experimental

2.1. Specimens

The polymer used in this study was polystyrene obtained in the form of $\frac{7}{8}$ in. diameter extruded rod (M_n = 104 100; M_w = 245 400; M_w/M_n = 2.356; a general purpose commercial grade from the Dow Chemical Co). After machining, specimens were carefully polished to minimize possible surface effects on the mechanical behaviour and then annealed following the method of Bailey [20].

The specimen geometry shown in Fig. 1a was specially designed since preliminary tests showed that most fractures occurred in the thread or

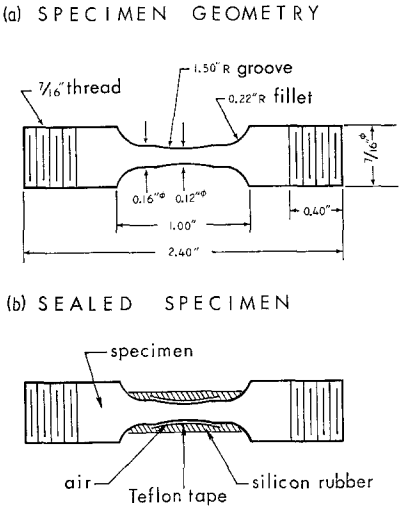

Figure 1 (a) Sample geometry; all dimensions are in inches. (b) Sealed specimen.

fillet parts. The cross-section at the thread was made as large as possible and the diameter was reduced at the centre section of the gauge lengths in order to control fracture at a given location for optical observation. By using Bridgman's method [21], the stress distribution in the grooved part was analysed. It was estimated that the radial and tangential components produced by the existence of the groove was only about 1 % of the stress applied to longitudinal tensile direction. Therefore, in the data analysis, these small quantities were neglected as experimental error.

Sealing of a specimen was performed as shown in Fig. 1b. First, a Teflon tape was wrapped tightly around the gauge length to protect the specimen from environmental effects. Then, to hold the entire assembly, a transparent silicon rubber (RTV 108 from General Electric) was attached and cured at room temperature for at least 1 day. During this procedure, great care must be exercised in the handling of the specimen

to avoid any adsorption of skin oil which is a crazing agent for polystyrene. According to Paterson's data [22], silicon rubber exhibits its glass transition at room temperature at about 4.3 kbar, such a seal would remain in the rubbery state and would not be expected to interfere with the experimental observations.

2.2. Apparatus and procedures

The apparatus used in this study, which has been described previously elsewhere [23], is essentially a constant cross-head speed tensile machine contained within a pressure chamber filled with a pressure-transmitting fluid. Pressure can be maintained at a selected constant value during specimen straining. The specimen holders were designed so as to allow all parts of the specimen to be in contact with the pressurizing fluid thereby applying a truly hydrostatic pressure to the sample. The tensile load applied to the specimen was measured by a pressure-compensating load cell within the pressure chamber. Strain was monitored both from the "cross-head travel" at the movable end of the specimen by means of a linear transducer and by measuring the reduction in the area at gauge lengths from direct photographic observation through windows. The latter photographic method was most useful in determining true stress-strain curves especially after sample necking.

Silicon oil (Dow Corning 200) was used as a pressure-transmitting fluid and the tensile tests were conducted at constant cross-head speed of $1.30 + 0.15\%$ min^{-1} and at temperature of $31 \pm 1°C$.

To obtain true stress-strain curves for sealed specimens the following procedure was taken. After complete fracture of the polystyrene some force due to the intact connected rubber seal, as shown in Fig. 2, was still observed. The true force applied to specimen was calculated simply by subtracting the force due to rubber from the observed total force.

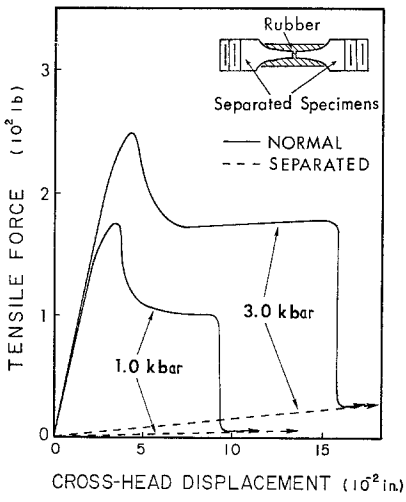

Figure 2 Tensile force versus cross-head displacement curves for sealed specimen (solid line) and separated specimen (dashed line) at 1.0 and 3.0 kbar.

3. Results

3.1. Environmental effect

In mechanical experiments under hydrostatic pressure, test specimens are immersed in pressure-transmitting fluids which, unfortunately, in nearly all cases are environmental crazing and cracking agents for glassy polymers.

Environmental effects on mechanical behaviour by silicon and castor oils, which are considered to be fairly inactive for polymers and often used as a pressure transmitting fluid, can be observed even at atmospheric pressure, as shown in Fig. 3. The specimen tested in air showed in inflection point on the stress-strain curve indicating the initiation of craze formation. Very similar stress-strain curves have been observed by Hoare and Hull [24] and Rabinowitz *et al.*[25]. From optical observations during straining, they found that crazes appear at the stress level which corresponds to the inflection and that an extensive craze development begins at the maximum point on the stress-strain curve. Therefore, the stress which corresponds to the inflection is defined as the "craze initiation"

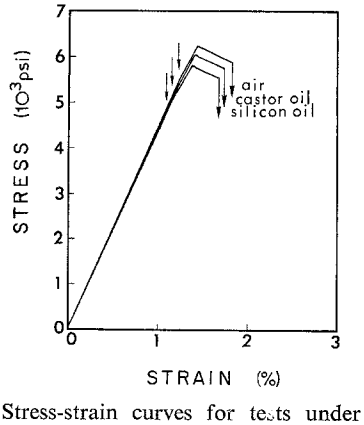

Figure 3 Stress-strain curves for tests under various environmental conditions at atmospheric pressure. Arrows indicate an inflection point on the stress-strain curve.

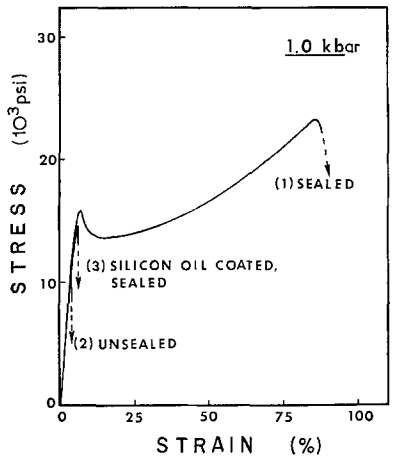

Figure 4 Stress-strain curves under different surface conditions at 1.0 kbar; (1) sealed specimen, (2) unsealed specimen tested in silicon oil, (3) specimen, whose surface was coated with silicon oil and then sealed.

stress while the maximum stress is called the "craze yielding" stress. Specimens tested in silicon and castor oil showed similar stress-strain curves. These environmental fluids caused a measurable lowering of craze initiation, craze yielding and fracture stresses.

Much more significant environmental effects were observed at higher pressure. In Fig. 4, the stress-strain curve for a sealed specimen tested at 1.0 kbar showed very ductile behaviour. By contrast, the unsealed specimen tested in silicon oil showed a brittle fracture at very low stress and strain levels. When the surface of specimen was coated with a thin layer of silicon oil and then sealed with Teflon tape and rubber, the stress-strain curve still showed brittle fracture but the fracture stress was much higher than that of the unsealed specimen. Similar experiments were performed at 3.0 kbar (Fig. 5). Both sealed and unsealed specimens showed ductile fracture. However, silicon oil and even skin oil which was simply applied by rubbing the surface of specimen by hand before sealing, lowered the ductile fracture stress.

All these experiments clearly showed that silicon oil drastically changes the mechanical properties of polystyrene under pressure. Similar effects on polymethylmethacrylate using a 50/50 mixture of castor oil and hydraulic pressure fluid have been reported by Harris *et al.* [26] who found that a surface coating also prevented brittle fracture. It should be noted that almost all previous experiments on mechanical properties of crystalline and amorphous polymers under pressure were carried out without sealing of test specimen from the environmental fluid, and undoubtedly, the reported data were affected by the pressure transmitting medium.

3.2. Stress and strain behaviour

Systematic tensile tests under pressure were performed for both sealed and unsealed samples using silicon oil as the pressure transmitting fluid. Fig. 6 shows typical stress-strain curves for unsealed specimens. Craze yielding was

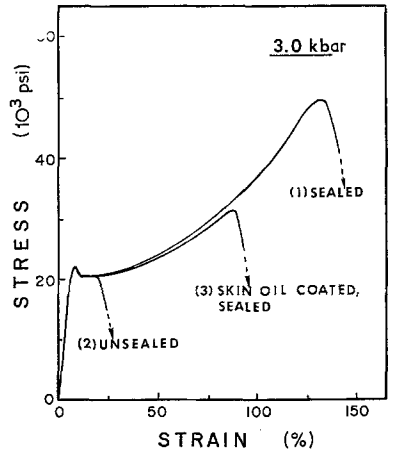

Figure 5 Stress-strain curves under different surface conditions at 3.0 kbar; (1) sealed specimen, (2) unsealed specimen tested in silicon oil, (3) specimen, whose surface was coated with skin oil and then sealed.

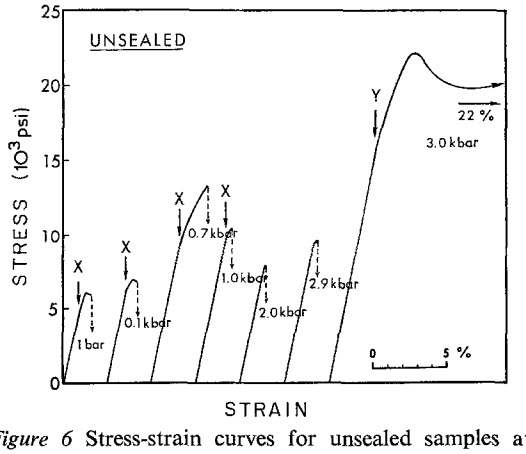

Figure 6 Stress-strain curves for unsealed samples at various pressures. Inflection points indicated by arrows X and Y correspond to craze initiation and shear band initiation points, respectively.

observed up to 0.1 kbar but above this pressure the fracture occurred in more brittle manner without the craze yielding. The fracture stress increased with pressure up to 0.7 kbar and then decreased. Inflection points indicated by arrows X, which correspond to craze initiation, could be seen up to 1.0 kbar. Samples tested above 1.2 kbar fractured suddenly without such an inflection point on the stress-strain curve. A drastic change appeared between 2.9 and 3.0 kbar, where the fracture mode changed from brittle to ductile. Pugh *et al.* [3], who performed similar tensile tests on polystyrene in castor oil, reported a quite similar discontinuous brittle to ductile transition at about 2.8 kbar. On the stress-strain curves for ductile fracture, an inflection point similar to the case of brittle fracture was detected as indicated by arrow Y. It has been shown by Kramer [28] that the stress at the inflection point corresponds to the initiation stress of diffuse shear bands. When the test specimens were sealed, the observed stress-strain curves shown in Fig. 7 were very different.

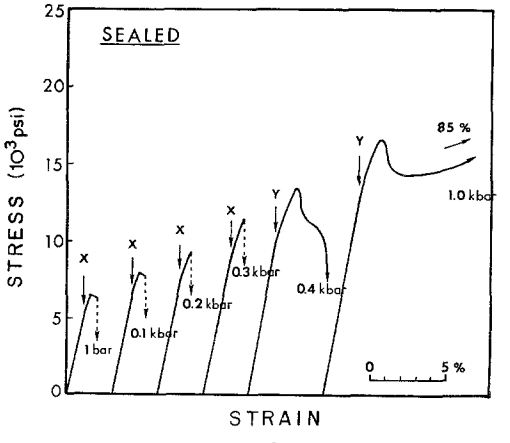

Figure 7 Stress-strain curves of sealed samples at various pressures. Inflection points indicated by arrows X and Y correspond to craze initiation and shear band initiation points, respectively.

The fracture stress increased continuously with pressure and the brittle-to-ductile transition occurred in a much lower pressure region between 0.3 and 0.4 kbar. Above this transition pressure, the fracture strain also increased considerably with pressure. The fracture stress for brittle fracture and upper yield stress for ductile fracture for both unsealed and sealed specimens are expressed as a function of pressure in Fig. 8. These curves show dramatically the environmental effect on the brittle to ductile transition. It is interesting to note that this observation is quite different from that by Pugh *et al.* [3], who reported that samples sealed with rubber showed a brittle to ductile transition at almost the same pressure of 2.8 kbar as unsealed samples. This discrepancy might originate from different experimental factors, since all of their sealed samples failed in the uncovered thread region below the transition pressure.

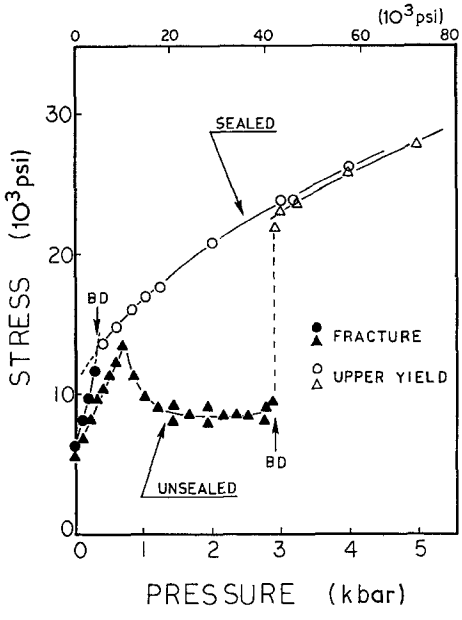

Figure 8 Pressure dependencies of fracture and upper yield stress in sealed and unsealed specimens. Arrows BD indicate the brittle-to-ductile transition.

4. Analysis and discussion

4.1. Brittle-to-ductile transition

Fig. 9 shows the pressure dependencies of craze initiation, shear band initiation, brittle fracture, and upper yield stresses for sealed specimens obtained from the stress-strain curves. By subtraction of hydrostatic stress component from these observed tensile stresses (σ_T), the pressure dependencies of the principal stresses ($\sigma^1 = \sigma_T - P$), whose directions are parallel to the tensile direction, are calculated and shown in Fig. 10.

The craze initiation stress has much higher pressure dependence than the shear band initiation stress, as shown in Fig. 9. This difference in the pressure dependencies is probably due to the fact that craze initiation

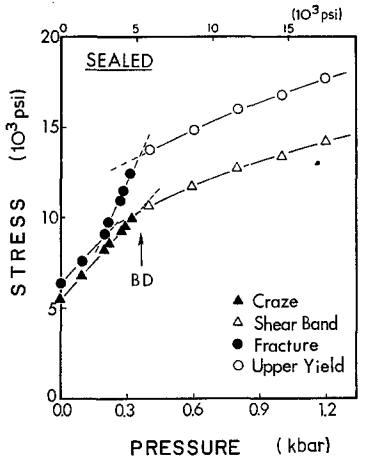

Figure 9 Pressure dependencies of craze initiation, shear band initiation, fracture, and upper yield stress in sealed specimen. Arrow BD indicates the brittle-to-ductile transition.

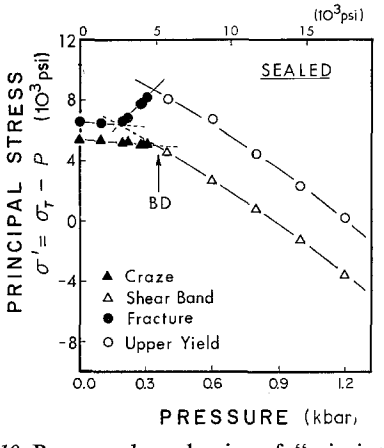

Figure 10 Pressure dependencies of "principal" craze initiation, shear band initiation, fracture, and upper yield stress in sealed specimen. Arrow BD indicates the brittle-to-ductile transition point.

involves a dilational void formation while shear band initiation requires no volume change. It is clear that the brittle-to-ductile transition occurs at the intersection of the two curves for craze and shear band initiation at the pressure indicated by the arrow (BD) in Figs. 9 and 10. Above the transition pressure, shear bands initiate at lower stress levels than crazes and as a result, the specimens shows higher ductility without any interruption by profuse crazing thus preventing cracking and fracture at low elongation.

From microscopic studies on the interaction of crazes and shear bands, it has been suggested by several groups including Bucknell *et al.* [29], Higuchi and Ishii [30] and Wellinghoff and Baer [31] that the shear bands function as craze "stoppers" as well as localized regions for energy absorption. One can apply shear banding as a prevention of craze formation and propagation to explain the change in the fracture modes from brittle fracture with craze yielding to brittle fracture without craze yielding which was observed between 0.1 and 0.2 kbar (see Fig. 7). In the specimens tested at 0.2 and 0.3 kbar, fracture surfaces of specimens examined in the optical microscope showed that the extensive development of crazes was suppressed by shear bands which were formed before craze yielding, and, subsequently, the specimens fractured at higher stress levels. A similar criterion for the pressure-induced brittle-to-ductile transition was proposed by Sternstein and co-workers [4, 5]. However, they defined this transition at the pressure where the curves for stresses of the normal stress yielding (corresponds to "craze initiation" in this paper) and shear yielding (corresponds to "upper yield") intersect. Our present study shows that the intersection of craze initiation and upper yield stress curves occur at much higher pressure than the actually observed brittle-to-ductile transition pressure (see Figs. 9 and 10).

Fig. 11 shows pressure dependencies of craze and shear band initiation stresses in addition to brittle and upper yield stresses for the unsealed

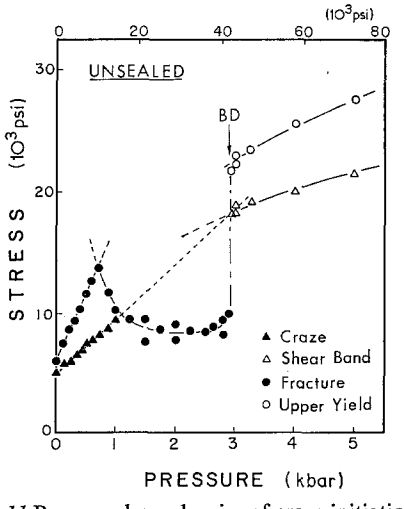

Figure 11 Pressure dependencies of craze initiation, shear band initiation, fracture, and upper yield stress in unsealed specimen. Arrow BD indicates the brittle-to-ductile transition.

measurements. The craze initiation stress increases almost linearly with pressure and intersects with the fracture stress curve at about 1.1 kbar. The extrapolated curve crosses the shear band initiation stress curve at almost the same pressure where the brittle-to-ductile transition was observed. The fracture surfaces examined with an optical microscope revealed a good correlation with the stress-strain behaviour. Fracture surfaces of specimens which were tested below 1.1 kbar showed a dense craze zone around the outside surface of the tensile specimen with evidence of crack initiation from the edge of the craze zone. However, those tested above 1.1 kbar showed no visible crazes, and the crack started directly from the outer surface. The fracture surfaces became more smooth with increasing pressure, indicating that crack propagation velocity was accelerated.

It has not yet been established why the unsealed specimen showed a discontinuous brittle-to-ductile transition at 2.95 kbar. The extrapolated curve showed that the pressure dependency of the craze initiation stress intersected with the shear band initiation stress curve at about 2.9 kbar (Fig. 11). It follows that the unsealed specimen also is expected to show the brittle-to-ductile transition at this pressure in the similar fashion as observed in the case of sealed specimen. A sharp transition actually occurred "discontinuously" at this pressure, probably due to the fact that a completely brittle fracture mode was observed in the pressure range from 1.1 to 2.9 kbar. In tensile experiments with polystyrene at atmospheric pressure, Hoare and Hull [24] found that a few localized crazes formed at the specimen surface at stress levels which were much lower than the stress corresponding to the inflection point on the stress-strain curve. If a similar craze formation occurred under pressure, such an imperfection could rapidly develop into a crack under high pressure with the aid of the environmental fluid. Such a crack could propagate at very high velocities causing a catastrophic brittle behaviour. But above the transition pressure, shear bands will form at a lower stress level than crazes thus preventing such craze formation and catastrophic fracture at very low strain. To better explain this unusual phenomenon, further studies are being conducted under pressure particularly emphasizing environmental effects on the craze initiation and the crack propagation processes.

4.2. Craze initiation criterion

The pressure dependencies of craze initiation stresses for both sealed and unsealed specimens, which have been already shown separately in Figs. 9 and 11, are amplified in Fig. 12a. As

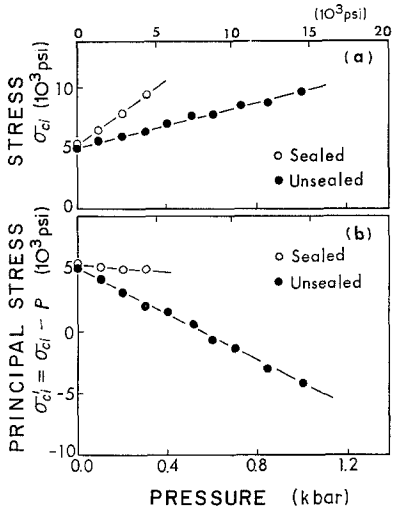

Figure 12 Pressure dependencies of (a) the craze initiation stress, σ_{ci}, and (b) the principal craze initiation stress, $\sigma_{ci}^1 = \sigma_{ci} - P$, in sealed and unsealed specimens.

already described, the craze initiation stresses were observed up to the brittle-to-ductile transition pressure for the sealed specimen and up to 1.0 kbar for the unsealed specimen. In both cases, a virtually linear pressure dependency of craze initiation stress was observed; however, the slope for unsealed specimens is much smaller. These two lines can be expressed numerically as

$$\sigma_{ci}(P) = 5.6 + 0.95P\ (\times 10^3\ \text{psi})\ \text{sealed}$$
$$= 5.1 + 0.32P\ (\times 10^3\ \text{psi})\ \text{unsealed}$$

or in a simple general form under constant temperature and strain rate by

$$\sigma_{ci}(P) = \sigma_0 + KP\ (0 < K \leqslant 1)$$

where $\sigma_{ci}(P)$ and σ_0 are craze initiation stresses at pressure P and at atmospheric pressure, respectively, and the pressure coefficient K indicates the degree of environmental effect, a small value indicating a strong effect.

Principal craze initiation stresses, $\sigma_{ci}^1 = \sigma_{ci} - P$, for both cases are shown in Fig. 12b as a function of pressure. It should be noted that the principal craze initiation stress for sealed

specimens shows almost no pressure dependency. This means that crazes initiate under hydrostatic pressure when the principal stress level reaches a critical value irrespective of ambient pressure. Therefore, if there is no environmental effect, the craze initiation criterion suggested from this study can be expressed as

$$\sigma_{ci}{}^{1} = \sigma_{ci} - P \simeq \text{constant}.$$

Another interesting observation is that crazes occurred even when $\sigma_{ci}{}^{1} < 0$ for the unsealed case, implying craze formation in a compressive stress field.

Craze initiation criteria under multiaxial stress state have previously been proposed and the validity of these relations will now be tested with the present data, as described below. From crazing studies of polymethylmethacrylate under biaxial stress fields (tension–tension [4] and torsion–tension [5]) Sternstein and his co-workers proposed the craze initiation criterion

$$\sigma_b = |\sigma^1 - \sigma^3| \geqslant A(T) + \frac{B(T)}{I_1}$$

where σ_b is a "stress bias" having a magnitude equal to the largest difference of the principal stresses, $A(T)$ and $B(T)$ are temperature dependent material constants, and $I_1 = \sigma^1 + \sigma^2 + \sigma^3$ is the first stress invariant in the principal stress field. In the case of tensile tests under pressure P, the three principal stresses are $\sigma^1 = \sigma_T - P$, $\sigma^2 = -P$, and $\sigma^3 = -P$, and so $I_1 = \sigma_T - 3P$. They also suggest that the craze formation requires a dilational stress field ($I_1 > 0$), in other words, that crazes never form in the stress field of $I_1 \leqslant 0$.

As a result of biaxial compression-tension experiments, Oxborough and Bowden [6] recently proposed a similar craze initiation criterion in terms of critical strain,

$$\epsilon_{ci} = \frac{X'}{I_1} + Y'$$

where X' and Y' are time- and temperature-dependent parameters. A different type craze initiation criterion has been proposed by Gent [7] who suggested that craze formation in glassy polymers occurs in two stages; a local transformation from a glassy state to a soft rubbery phase, and cavitation of the rubbery phase under dilatant stress. His criterion is given by

$$\sigma_{ci} = 3[\beta(T_g - T) + P]/k$$

where β is a hydrostatic pressure cofficient of T_g and k the stress concentration factor at the flaw tip. From material constants $\beta(T - T_g) = 44 \times 10^3$ psi and by assuming $k = 20$, he predicted the pressure dependency of craze initiation stress in polystyrene as

$$\sigma_{ci} = 6.5 + 0.15P\ (\times 10^3 \text{ psi})$$

and obtained good fit to Biglione's experimental data [3]. Unfortunately, Biglione reported only fracture stresses for unsealed polystyrene specimens which were, of course, affected by the environment; experimental data on the craze initiation stress was not presented.

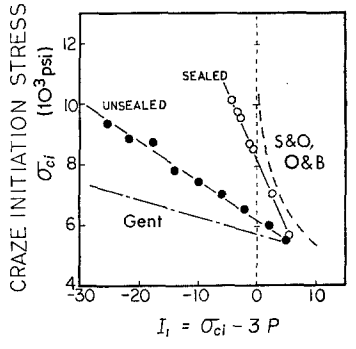

Figure 13 Comparison of experimental data with craze initiation criteria as predicted by Sternstein and Ongchin [4] (S & O) and Oxborough and Bowden [6] (O & B), and Gent [7].

In Fig. 13, the experimental data obtained in this study are plotted to check these criteria. The craze initiation stress is plotted against the first stress invariant and compared with the craze initiation criteria described above. Sternstein and Ongchin's and Oxborough and Bowden's criteria are quite similar and are expressed qualitatively by the same line, although σ_{ci} in the figure should be alternated with ϵ_{ci} in the latter criterion. The experimental data for both sealed and unsealed specimens fall on almost linear lines with different slopes due to the environmental effect. Only Gent's criterion is linear but the slope of the predicted line is too small. The other criteria predict a non-linear curve and that crazing does not occur when $I_1 < 0$.

These discrepancies between our experimental data and the craze initiation criteria deduced from biaxial stress experiments might be related to problems in the procedures used during biaxial experimentation.

In our case of tensile deformation under

hydrostatic pressure, the specimen is strained after the application of a preselected hydrostatic pressure, that is, from an isotropically compressed state. However, in biaxial stress experiments, one of the stress components such as tension, torsion, or compression is usually applied first and then the craze formation is examined by varying the magnitude of the second stress component normally applied in tension. Therefore, when examining the craze initiation condition in biaxial stress fields, the stress state of the specimen is never isotropic prior to the application of tension. Unfortunately, it seems that previous biaxial experiments were not carried out with the conscious recognition of this problematic situation. One critical case probably affected by this situation is illustrated in Fig. 14 and explained below.

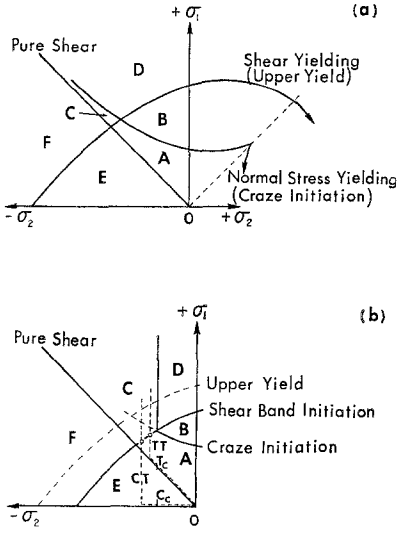

Figure 14 (a) The second quadrant behaviour suggested by Sternstein and Myers [5]. The stress states A and E are zones of no yielding in any form; C and F, are zones of shear yielding only; B, is a zone of crazing only; and D, is a zone of both crazing and shear yielding. (b) Revised second quadrant behaviour. The symbols A to F denote the same zones as (a). The paths TT and CT show the transformation of stress state during torsion–tension and compression–tension experiments. T_c and C_c indicate critical values in the experiments.

Sternstein and Myers [5] have stated that four distinct types of material response can be seen in the second quadrant stress fields, depending on the stress levels as shown in Fig. 14a. Stress states in regions A and E produce no yielding in any form; C and F, shear yielding but no crazing; B, crazing but no shear yielding; and D, both crazing and shear yielding (see Fig. 9 in [5]). In this sectioning of stress fields from A to F, two important factors were not considered. The interaction of shear bands and crazes described in Section 4.1, and the sequential loading procedure in biaxial tests discussed just before. Both of these factors could change the position of the regions shown in Fig. 14a, expecially region D, as is shown in Fig. 14b. In the figure, our terms of "upper yield" and "craze initiation" are employed instead of "shear yielding" and "normal stress yielding". The shear band initiation curve is drawn using the assumption that shear bands initiate at stress level roughly $\frac{3}{4}$ to $\frac{4}{5}$ of upper yield stress. For example, consider the progression of stressing in torsion–tension along the path indicated by TT in Fig. 14b and in compression–tension along the path CT. If the initially applied torsion or compression stress is lower than a critical value of T_c or C_c indicated in the figure, the specimen in region D will contain both crazes and shear bands if the specimen does not fracture before the initiation of the shear bands. Also if the applied stress is higher than T_c or C_c, shear bands will initiate first and the formation of crazes will be suppressed. Even though the crazes may form due to poor shear band development, the macroscopically observed stress for craze formation may be higher than the craze initiation stress which is normally observed in the material without shear bands due to suppressional function of pre-existing shear bands. Nevertheless, the craze initiation process affected by pre-formed shear bands could be studied in the type of experimental arrangement used by Sternstein and Myers and Oxborough and Bowden. Another experimental problem could have occurred in the Sternstein and Ongchin experiment. Silicon oil was used to produce a tangential tensile component in their biaxial tension–tension experiment with polymethylmethacrylate. Our recent observations have shown that silicon oil acts as a stress crazing agent on polymethylmethacrylate as well as polystyrene, and subsequently, it may be possible that the reported values for craze initiation were affected by the silicon oil environment.

To further discuss the craze initiation criteria in the biaxial stress fields, it is highly desirable to check and improve the experimental problems discussed above.

4.3. Yield criteria

When compared with craze initiation, yield criteria under combined stresses and hydrostatic pressure has been studied more extensively. To take into account the significant effect of hydrostatic pressure on the yield in polymers, simple yield criteria, such as the Tresca criterion, $\tau_{max} = |\sigma^1 - \sigma^3| =$ constant, and the von Mises criterion, $\tau_{oct}^2 = (\sigma^1 - \sigma^2)^2 + (\sigma^2 - \sigma^3)^2 + (\sigma^3 - \sigma^1)^2 = \frac{2}{3} K^2$ where K^2 is the second stress invariant, have been modified in several ways. The Coulomb yield criterion [10], which originally was applied to soil, is a pressure modified Tresca criterion

$$\tau_{max}(P) = \tau_0 - \mu\sigma_m .$$

Also, a pressure modified von Mises criterion can be expressed in the form

$$\tau_{oct}(P) = \tau_0' - \mu'\sigma_m$$

where $\tau_{max}(P)$ and $\tau_{oct}(P)$ are the maximum shear stress and the octahedral shear stress at pressure P, τ_0 and τ_0' are these stresses at atmospheric pressure, μ and μ' are material parameters describing the pressure dependency of the respective yield stresses, and $\sigma_m = (\sigma^1 + \sigma^2 + \sigma^3)/3$ is the mean normal stress.

The application of the Coulomb criteria to polymers under uniaxial and biaxial stress fields has been performed by Whitney and Andrews [8] and Bowden and Jukes [9], and Sternstein and Ongchin [4] have successfully applied the modified von Mises criteria. A similar relation including temperature and rate effects, $\tau_0' + AP = f(\dot{\epsilon}, T)$ where A is constant and $\dot{\epsilon}$ is the strain rate, has been proposed by Bauwens [11]. For tension under hydrostatic pressure, where the principal stresses are expressed as $\sigma^1 = \sigma_T - P$, $\sigma^2 = \sigma^3 = -P$, these two pressure modified criteria give a similar linear pressure dependency and no difference between the two criteria was observed. Similarly, Rabinowitz *et al.* [32] measured the pressure dependency of the shear yield behaviour in polymethylmethacrylate and showed that the data could be expressed by a similar relation of the form $\tau(P) = \tau_0 + AP$.

Fig. 15 shows the Mohr circle diagram of yield stresses for sealed specimens. The envelope of the Mohr circles shows a slight curve; a straight line of common tangent as predicted by any of the yield criteria described above does not exist. Recently, a different type of pressure modified von Mises criterion, whose original form was proposed by Schleicher [33] and which gives a non-linear pressure dependency on the yield stress, was demonstrated by Raghava *et al.* [12] to fit experimental data in various stress fields. We shall call this criterion a "non-linear" pressure dependent von Mises criterion to distinguish the previous one, a "linear" pressure dependent von Mises criterion. In the case of tension test under hydrostatic pressure, the difference in the two kinds of modified von Mises criteria can be demonstrated most significantly by the following normalized forms [12],

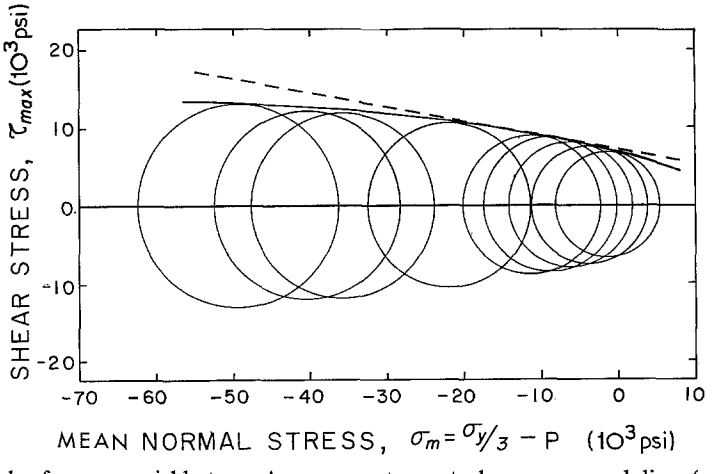

Figure 15 Mohr-circles for upper yield stress. A common tangent shows a curved line (solid line). The dotted straight line is the extrapolated line of common tangent from the lower pressure region.

$$R = 1 + \frac{3}{2} B \left(\frac{X-1}{X}\right)$$

$$R = -\left(\frac{X-1}{2}\right) + \frac{1}{2}\left[(X+1)^2 + 12B(X-1)\right]^{\frac{1}{2}}$$

where $R = \sigma_T/T$, $X = C/T$, $B = P/T$, and C and T are the compressive and tensile yield stresses at atmospheric pressure. Since compression measurements were not carried out in this study, the value of C employed was from the work of Binder and Muller [34] and Haward [35], while the value of T was obtained by extrapolation of the yield stresses observed under pressure to atmospheric pressure.

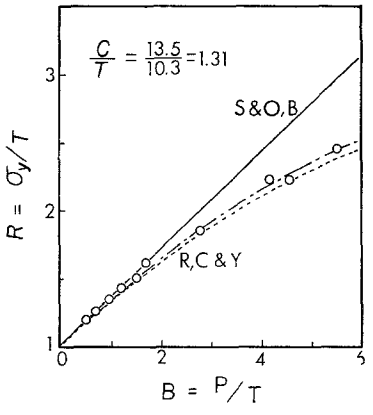

Figure 16 Comparison of experimental data with theoretical yield stress values predicted by Sternstein and Ongchin [4] (S & O) and Bauwens [11] (B), and by Raghava *et al.* [12] (R, C & Y).

The experimental data are compared in Fig. 16 with the values predicted by the linear and non-linear pressure dependent von Mises criteria. At low pressures the difference in predicted values between the two criteria is small. However, at higher pressures the experimental data show much better agreement with the non-linear pressure dependent von Mises criterion. The stress range which biaxial experimentation can cover is limited due to the nature of the experiment, so that the data from these types of measurements could be fitted by either of the von Mises criteria within experimental error. For this reason, either tensile or compression tests under pressure are more powerful experimental tools for elucidating the validity of proposed yield criteria. As seen above, the non-linear pressure dependent von Mises criterion gives the best fit to the experimental data using only the two parameters of C and T, which can be obtained by experiments at atmospheric pressure.

4.4. Ductile fracture criterion

Fig. 17 shows the pressure dependency of the fracture stress for both sealed and unsealed samples. Above the brittle-to-ductile transition

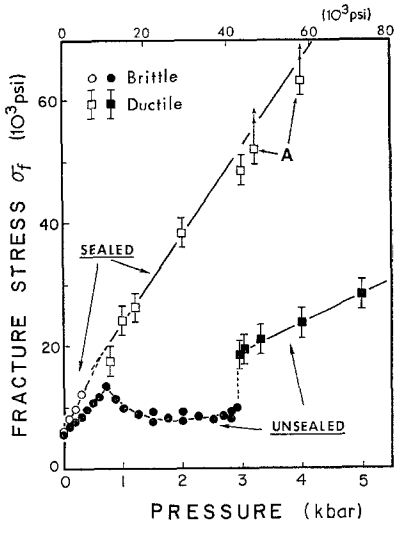

Figure 17 Pressure dependencies of brittle and ductile fracture stress in sealed and unsealed specimens. (Arrows A indicate samples which did not break due to limitations in cross-head travel.)

pressure, the ductile fracture stress for sealed specimen increased almost linearly with pressure and at 4.0 kbar was over ten times of the fracture stress observed at atmospheric pressure. In contrast, the unsealed samples showed a much lower fracture stress due to the environmental effect. It is particularly interesting that this effect caused the lowering of fracture stress even in the ductile fracture region.

In Fig. 18, the principal ductile fracture stress and the principal craze initiation stress for both sealed and unsealed specimens are plotted as a function of pressure. The principal ductile fracture stress for sealed specimens shows almost no pressure dependency within experimental error as well as the principal craze initiation stress, suggesting that ductile fracture occurs when the principal stress level on the specimen reaches a critical value regardless of the applied pressure. In the case of metals, Pugh [36] found that the same criterion could be applied to annealed copper tested under pressure.

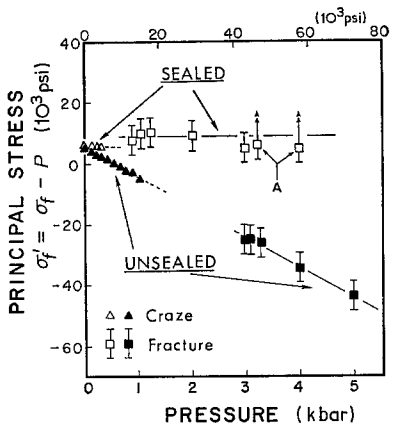

Figure 18 Pressure dependencies of principal craze initiation and ductile fracture stress in sealed and unsealed specimens. (Arrows A indicate samples which did not break due to limitations in cross-head travel.)

It is surprising to observe that a similar pressure dependency exists between the craze initiation and the ductile fracture processes in both sealed and unsealed specimen. These correlations suggest that the stress state required for the craze initiation and the ductile fracture processes are quite similar and the governing factor seems to be the first principal tensile stress. Also, the environmental effect on these processes is amplified equally with increasing applied pressure. On the other hand, the yielding process, which occurs by shear deformation behaved quite differently from the crazing and fracture processes. The yield stress increased non-linearly with increasing pressure and was hardly affected by the environment.

5. Conclusions

Tensile experiments on polystyrene under pressure showed that the mechanical properties of polystyrene are strongly affected by silicon oil. Studies on sealed specimens enabled us to elucidate the mechanism of the brittle-to-ductile transition and to observe the experimental criteria for the craze initiation, yielding, and ductile fracture processes.

The major conclusions of this study may be summarized as follows:

(1) Silicon oil used as a pressure-transmitting fluid functions as a stress crazing and cracking agent under pressure. This environmental effect lowers the craze initiation and ductile fracture stress, while causing little change on upper yield stress.

(2) The craze and shear band initiation stresses have different pressure dependency curves which intersect at the brittle-to-ductile transition pressure. Above the transition pressure, shear bands initiate at a lower stress level than crazes, thereby preventing craze formation.

(3) The principal craze initiation stress shows almost no pressure dependency, suggesting that crazes initiate when the principal stress level reaches a critical value irrespective of the applied pressure.

(4) The pressure dependency of the yield stress agrees well with a non-linear pressure dependent von Mises yield criterion rather than a linear pressure dependent von Mises or Coulomb yield criteria.

(5) The principal stress for ductile fracture has almost no pressure dependency and behaves qualitatively like the craze initiation process showing a similar pressure dependency and response to environmental effects.

Acknowledgements

This research was generously supported by the Office of Naval Research. Special thanks are due to Dr F. W. G. Fearon for his advice and to Dow Corning who supplied us with silicon oil.

References

1. L. HOLLIDAY, J. MANN, G. A. POGANY, H. PUGH and D. A. GUNN, *Nature* **202** (1964) 381.
2. H. PUGH, E. F. CHANDLER, L. HOLLIDAY and J. MANN, *Polymer Eng. Sci.* **11** (1971) 463.
3. G. BIGLIONE, E. BAER and S. V. RADCLIFFE, in "Fracture 1969" Proceeding of the Second International Conference, Brighton, 1969, edited by P. L. Pratt (Chapman and Hall, London, 1969).
4. S. S. STERNSTEIN and L. ONGCHIN, *A.C.S. Polymer Preprints* **10** (1969) 1117.
5 S. S. STERNSTEIN and F. A. MYERS, *J Macromol. Sci. Phys.* **B8** (1973) 557.
6. R. J. OXBOROUGH and P. B. BOWDEN, *Phil. Mag.* **28** (1973) 547.
7. A. N. GENT, *J. Mater. Sci.* **5** (1970) 925.
8. W. WHITNEY and R. D. ANDREWS, *J. Polymer Sci.* **C16** (1967) 2981.
9. P. B. BOWDEN and J. A. JUKES, *J. Mater. Sci.* **3** (1968) 183.
10. C. A. COULOMB, *Mém. Math. et Phys.* **7** (1773) 343.
11. J. C. BAUWENS, *J. Polymer Sci.* **A-2 8** (1970) 893.
12. R. RAGHAVA, R. M. CADDELL and G. S. Y. YEH, *J. Mater. Sci.* **8** (1973) 225.
13. D. R. MEARS, K. D. PAE and J. A. SAUER, *J. Appl. Phys.* **40** (1969) 4229.
14. L. A. DAVIS and C. A. PAMPILLO, *ibid* **42** (1971) 4659.

15. A. W. CHRISTIANSEN, E. BAER and S. V. RADCLIFFE, *Phil. Mag.* **24** (1971) 451.
16. J. A. SAUER, D. R. MEARS and K. D. PAE, *Eur. Polymer J.* **6** (1970) 1015.
17. W. I. VROOM and R. F. WESTOVER, *SPE J.* **25** (1969) 58.
18. D. SARDAR, S. V. RADCLIFFE and E. BAER, *Polymer Eng. Sci.* **8** (1968) 290.
19. S. B. AINBINDER, M. G. LAKA and YU. I. MAIRORS, *Mekkanika Polemerov* **1** (1965) 65.
20. J. BAILEY, *Modern Plastics* **24** (1946) 127.
21. P. W. BRIDGMAN, *Trans. ASM* **32** (1944) 553.
22. M. S. PATERSON, *J. Appl. Phys.* **35** (1964) 176.
23. G. DAS and S. V. RADCLIFFE, *J. Jap. Inst. Metals* **9** (1968) 334.
24. J. HOARE and D. HULL, *Phil. Mag.* **26** (1972) 443.
25. S. RABINOWITZ, A. R. KRAUSE and P. BEARDMORE, *J. Mater. Sci.* **8** (1973) 11.
26. J. S. HARRIS, I. M. WARD and J. S. C. PARRY, *ibid* **6** (1971) 110.
27. A. S. ARGON, R. D. ANDREWS, J. A. GODRICK and W. WHITNEY, *J. Appl. Phys.* **39** (1968) 1899.
28. E. J. KRAMER, *J. Macromol. Sci. Phys.* **B10** (1974) 191.
29. C. B. BUCKNELL, D. CLAYTON and W. E. KEAST, *J. Mater. Sci.* **7** (1972) 1443.
30. M. HIGUCHI and H. ISHII, *Repts. Res. Inst., Appl. Mech. Kyushu University* **16** (1968) 69.
31. S. WELLINGHOFF and E. BAER, to be published.
32. S. RABINOWITZ, I. M. WARD and J. S. C. PARRY, *J. Mater. Sci.* **5** (1970) 29.
33. F. SCHLEICHER, *Z. Agnew. Math. Mech.* **6** (1926) 199.
34. G. BINDER and F. H. MULLER, *Kolloid Z.* **177** (1961) 129.
35. R. N. HAWARD, B. M. MURPHY and E. F. T. WHITE, *J. Polymer Sci.* **A-2 9** (1971) 801.
36. H. PUGH, International Conference on Materials ASTM, Philadelphia USA, February 1964.

Received 30 September and accepted 14 November 1974